Supplementary Information

Numerical model

A force-based model of active cells was implemented to study emergence of collective rotation on rings of cells. A one-dimensional framework was used, modelling the ring as a segment with periodic boundaries associated to an *x*-axis.

Our model is entirely driven by explicit mechanical processes, with the single cell as the building block. Cells are segments of original length $2R_0 = 40\mu\mathrm{m}$, located using the position of their center on the *x*-axis. The use of a force-balance method allows the explicit tracking of individual cells. Cells are subject to three types of surface forces: viscous cell-substrate forces proportional to their velocity; elastic contact forces representing volume exclusion; and active forces.

Active forces are implemented as the sum of a noise $\boldsymbol{\eta}$, representing autonomous cell diffusion, and an effective persistent migration force $\boldsymbol{f_M}$. $\boldsymbol{\eta}$ is a 1D Gaussian noise of mean 0 and standard deviation σ. $\boldsymbol{f_M}$ strongly relates to cell polarization: cells in our model can be found in one of three polarity states (*S, CW* and *CCW*) representing their possible dynamical behaviors. The migration force f_M is equal to 0 for a non-persistently polarized cell, referred to as *static (S)* and exhibiting Brownian motion at the considered time scale; it is equal to $\pm F_M$, where F_M is a constant, for a persistently polarized cell in either direction, referred to as *clockwise (CW)*- or *counter clockwise (CCW)*-polarized.

The contact force caused by cell *i* on another cell is:

$$\boldsymbol{f_{c,i}} = F_C \left(1 - \frac{d_i}{2R}\right) 1_{\{2R-d_i\}} \boldsymbol{u}_i$$

where F_C is the cell stiffness, *R* the cell radius, d_i is the distance between both cells and $\boldsymbol{u}_i$ is the unit vector pointing from cell *i* to the other cell. $1_{\{x\}}$ is the Heaviside step function, equal to 1 if $x \geq 0$ and to 0 otherwise. F_c is an effective parameter representing the extent to which cells will react, reorient and change their behavior upon intercellular contact: it encompasses volume exclusion due to mechanical stiffness, but also biochemical parameters such as intercellular adhesion. The effect of cell stiffness on collective migration was also experimentally demonstrated in previous research work [1] and is reminiscent of our results described in Fig. 4g and Movie 10b.

Thus, the total balance of forces on a cell migrating on the ring with velocity $\boldsymbol{v}$ is:

$$\mu \boldsymbol{v} = \left(f_{C,i} - f_{C,j}\right)\boldsymbol{u} + \boldsymbol{f_M} + \boldsymbol{\eta}$$

where μ is the viscous friction coefficient, cells *i* and *j* are the nearest left-side and right-side cell neighbors respectively, and $\boldsymbol{u}$ is the unit vector pointing towards the positive *x*-axis.

[Desai et. al,2013, RSI] showed that CIL-associated cell repolarizations occur probabilistically, an observation we adopted in our model. In our model, the probability for a cell polarity to change is mechanically driven: it depends on the forces on this cell and is controlled by a force threshold F_0. Single isolated cells in experiments never get persistently polarized, indicating that $\boldsymbol{\eta}$ does not impact polarity changes. Moreover, repolarization requires intercellular contacts lasting a few minutes, indicating that an average force during a contact time τ_{int} is more likely to drive repolarization than a high, punctual force. Therefore, the probability for a cell to become persistently polarized at a given time *t* increases with $\frac{1}{F_0}\left|\int_{t-\tau_{int}}^{t} f(u)du\right| \equiv \frac{1}{F_0}\int f(t)$, where f is the projection of the sum of $\boldsymbol{f_M}$ and of contact forces on the cell. It is worth noting that persistent polarization seems to be irreversible: return to a *static* state is impossible.

For a cell in the polarity state *X* subjected to $\int f$, for a given time step *dt*, the probability distributions associated to polarity changes are given by:

$$\mathbb{P}(X \to CCW|\int f, dt) = 1 - \left(\frac{1}{1+e^{k_s\left(\frac{\int f}{F_0}-1\right)}}\right)^{\frac{dt}{\tau_{int}}} \underbrace{+\,\mathbb{P}_{remain}(CCW|\int f, dt)}_{\text{if } X=CCW}$$

$$\mathbb{P}(X \to CW|\int f, dt) = 1 - \left(\frac{1}{1+e^{-k_s\left(\frac{\int f}{F_0}+1\right)}}\right)^{\frac{dt}{\tau_{int}}} \underbrace{+\,\mathbb{P}_{remain}(CW|\int f, dt)}_{\text{if } X=CW}$$

$$\mathbb{P}(X \to S\,|\int f, dt) = \begin{cases} \mathbb{P}_{remain}(S|\int f, dt) \text{ if } X = S \\ 0 \text{ otherwise} \end{cases}$$

Where $\mathbb{P}_{remain}(X|\int f, dt) \approx \left(\frac{1}{1+e^{k_s\left(\frac{|\int f|}{F_0}-1\right)}}\right)^{\frac{dt}{\tau_{int}}}$ is a sigmoid function of steepness k_s.

Biophysical parameters were calibrated using experimental data. The persistent migration parameter $\frac{F_M}{\mu}$ was set using the average cell velocity during collective migration.

The cell diffusion parameter σ was adjusted using previous single cell literature. In 1D, the random motility coefficient of cells as defined in[2] is analogous to the cell diffusivity $\frac{1}{2}\left(\frac{\sigma}{\mu}\right)^2$ and equals S^2P where *S* is the root mean-squared cell velocity and *P* is the correlation time of cell direction. Literature for single MDCK cells provided us with orders of magnitude for S and P[3,4] and thus for σ relative to μ.

The parameters k_s and F_0 characterizing the probabilistic polarity changes were chosen so that the polarization time for a single cell hit by a 5 cell-train matches experimental values, and the probability for an isolated static cell to become persistently polarized is negligible. The cell stiffness $\frac{F_C}{\mu}$ was estimated by measuring cell compressibility in experiments of polarized cell trains migrating between obstacles (experimentally, obstacles were the borders of a non-continuous micro-pattern fibronectin ring) (**Supplementary Fig. 1a**). During the collective migration of a cell train towards the obstacle, the cell at the rear end of the train was seen to migrate unconstrained, with a radius *R*. When the front cell was stopped by the obstacle, the rear end cell continued migrating and got gradually compressed against the immobilized train (**Supplementary Fig. 1b**). Its velocity decreased until the cell stopped, with an equilibrium radius R_e (**Supplementary Fig. 1c,d**). Let us analyze the behavior of the rear end cell in terms of our model. Using force balance, we can deduce that $RF_M = (R - R_e)F_C$. By measuring experimental cell compression, we thus get an estimate of F_C relatively to F_M.

The model was implemented using Euler's method with a 24 second-timestep. Simulations were run up to 1 000 steps to reach a steady state.

Table of model parameters:

Parameter	Definition	Value
L	Ring perimeter	600 (μm)
R	Cell radius	20 (μm)
μ	Viscous friction	No data
F_M	Persistent motile force	8.3 10^{-9} μ (Pa)
σ	Cell diffusion parameter	4.5 10^{-8} μ (Pa)
F_C	Cell stiffness	4.6 10^{-8} μ (Pa)
τ_{int}	Contact time	60 (s)
k_s	Sigmoid steepness	~12
F_0	Force threshold	2.0 10^{-9} μ (Pa)

Coordination Time

The coordination time was defined as the duration between the last time of no preferential direction on the ring ($D = 0$) and the time when the coordination parameter reaches a final, lasting plateau at ±1, indicating complete coordination of the cells.

Correlation function

The spatial velocity correlation function was calculated for both experiments and simulations using the formula below:

$$C(x',t) = \frac{< u(x+x',t) \times u(x,t) >_x}{\sqrt{< u(x+x',t)^2 >_x \times < u(x,t)^2 >_x}}$$

where *x* and *x'* are curvilinear abscissas along the ring, *u* is the angular velocity (positive in the counter-clockwise direction) and *t* is time.

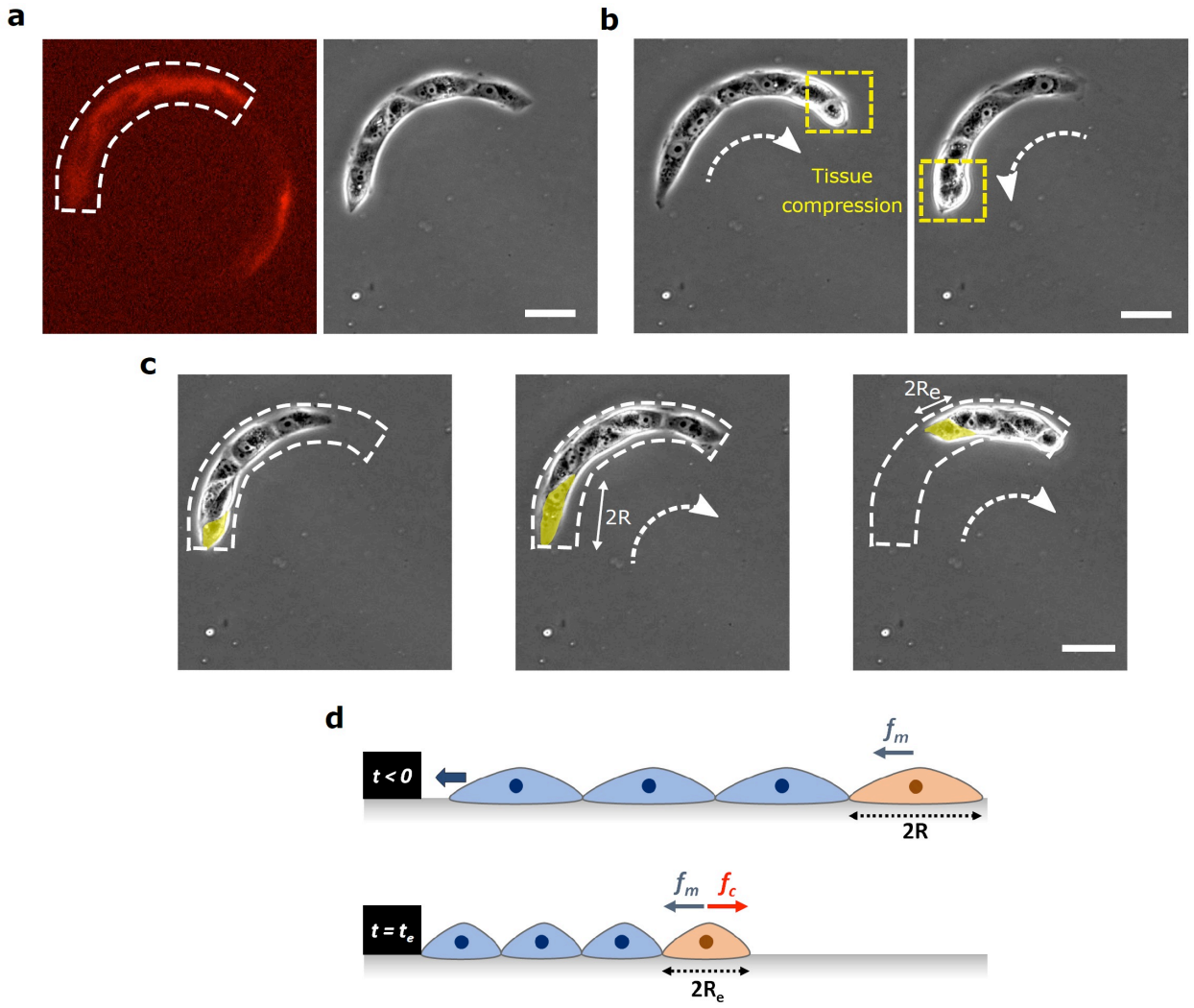

Supplementary Figure 1 | Cell compressibility measurement in experiments of polarized cell trains migrating between broken fibronectin micro-patterns.

a, Broken ring micro-patterns and cell train. **b,** Train migrating towards the end of fibronectin confinement: train at the point of maximal compression. **c,** Simulation parameter measurement of the resting radius *R* and equilibrium radius R_e of the last cell before and after compression as represented by a yellow shaded region. **d,** Schematic: force balance for the last cell of the train. All scale bars: 50 µm.

References:

1. Messica, Y. *et al.* The role of Vimentin in Regulating Cell Invasive Migration in Dense Cultures of Breast Carcinoma Cells. *Nano Lett.* **17**, 6941–6948 (2017).

2. Gail, M. H. & Boone, C. W. The Locomotion of Mouse Fibroblasts in Tissue Culture. *Biophys. J.* **10**, 980–993 (1970).

3. Li, Y. *et al.* Effect of scatter factor and hepatocyte growth factor on motility and morphology of mdck cells. *Vitro Cell. Dev. Biol. - Anim.* **28**, 364–368 (1992).

4. Pope, M. D. & Asthagiri, A. R. Short-Lived, Transitory Cell-Cell Interactions Foster Migration-Dependent Aggregation. *PLoS ONE* **7**, e43237 (2012).